

---

# Triangularity effects on the collisional diffusion for elliptic tokamak

**Pablo Martín\* and Enrique Castro**

Departamento de Física, Universidad Simón Bolívar,

Apdo. 89000, Caracas 1080A, Venezuela.

\* ) [pmartin@usb.ve](mailto:pmartin@usb.ve)

---

---

## Abstract

The effect of ellipticity and triangularity will be analyzed for axisymmetric tokamak in the collisional regime. Analytic forms for the magnetic field cross sections are taken from those derived recently by other authors. Analytic results can be obtained in elliptic plasmas with triangularity by using a special system of tokamak coordinates recently published. Our results show that triangularities smaller than 0.6 increases confinement for ellipticities in the range 1.2 to 2. This behavior happens for negative and positive triangularities, however this effect is stronger for negative than for positive triangularities. The maximum diffusion velocity is not obtained for zero triangularity, but for small negative triangularities. Ellipticity is also very important in confinement, but the effect of triangularity seems to be more important. High electric inductive fields increases confinement, though this field is difficult to modify once the tokamak has been built. The analytic form of the current produced by this field is like that of a weak Ware pinch with an additional factor, which weakens the effect by an order of magnitude. The dependence of the triangularity effect with the Shafranov shift is also analyzed.

---

---

## Introduction

The tokamaks (toroidal magnetic camera) seem to be the most promising alternative for the future fusion reactors on controlled nuclear fusion [1]. The nuclear fusion of the nuclei of deuterium and tritium produces  $\alpha$  particles (nuclei of helium), neutrons and energy, and in this process there is not heavy radioisotopes of large half-life. High temperature is required in order to produce this nuclear reactions in a large scale, which in the hydrogen bomb is obtained with a nuclear fission bomb. It is also required adequated densities and confinement time for the fuel particles in the thermonuclear fusion. The first tokamaks were toroides of circular cross sections, but the future generation of tokamaks (i.e. ITER) are like ellipses with triangularity and other types of deformation.

Most of the theories on confinement and instabilities were developed for circular cross sections at the beginning, but later the analysis were extended to more general configurations, mainly through computer simulations.

---

---

In this work plasma tokamak confinement is study for a general kind of plasma configurations including ellipticity and triangularity, as well as, nonlinear flows, in the low vorticity approximation. This new treatment seems suitable for the H-mode, where the existence of internal barriers and shear produce a large scale decreasing in turbulence. The analysis has been also extended to plasma configuration with current holes, since has been recently found that this particularity appears in most of the large tokamaks in operation.

It is interesting to point out that whilst vorticity, could be important within an internal barrier, however outside of the barrier, turbulence is low, and therefore vorticity, which is associated with turbulence, will be also low, then in some way can be neglected. Axisymmetric tokamaks will be considered here.

---

## THEORETICAL TREATMENT

The starting point is the steady state non-linear MHD equation

$$\rho \vec{v} \cdot \nabla \vec{v} = \frac{1}{c} \vec{j} \times \vec{B} - \nabla p ,$$

$$\vec{\omega} = \nabla \times \vec{v} ,$$

$$\vec{v} \cdot \nabla \vec{v} = \frac{1}{2} \nabla v^2 - \vec{v} \times \nabla \times \vec{v} ,$$

$$\rho \nabla F = \frac{1}{c} \vec{j} \times \vec{B} + \vec{\omega} \times \vec{v} ,$$

with the auxiliary function  $F$  defined as

$$F(\vec{v}, \rho, T) = \frac{v^2}{2} + W(\rho, T) ,$$

---

where  $W(\rho, T)$  is the enthalpy given by

$$W(\rho, T) = \int^{\rho} \frac{1}{\rho} \frac{\partial p}{\partial \rho} d\rho \quad .$$

This integral is performed along a magnetic line, where  $T$  can be considered constant, since as is well known, the heat transference along a magnetic lines is very fast. Now, if the vorticity is neglected then the previous equation becomes

$$\rho \nabla F = \vec{j} \times \vec{B} \quad ,$$

and from here

$$\vec{B} \cdot \nabla F = 0 \quad ,$$

---

This last equation shows that  $F(\vec{v}, \rho, T, \nu)$  is constant along a magnetic line, and therefore is constant on a magnetic surface, that is,

$$F(\vec{v}, \rho, T, \nu) = \tilde{F}(\psi) \quad ,$$

$$\nabla F(\vec{v}, \rho, T, \nu) = \frac{d \tilde{F}(\psi)}{d \psi} \nabla \psi \quad ,$$

where  $\psi$  is the well-known poloidal flux function. In the case where the geometrical orthogonal curvilinear coordinates  $(\tilde{\sigma}, \tilde{s}, \varphi)$  are used, the previous equation can also be written as

$$F(\vec{v}, \rho, T, \nu) = F(\tilde{\sigma}) \quad ,$$

$$\nabla F(\vec{v}, \rho, T, \nu) = \nabla F(\tilde{\sigma}) = - \frac{1}{h_{\sigma}} \frac{d F(\tilde{\sigma})}{d \tilde{\sigma}} = - \frac{\partial F(\tilde{\sigma})}{\partial \tilde{\sigma}} \hat{n} \quad ,$$

where  $h_{\sigma}$  is the corresponding scale factor in the curvilinear coordinates  $\tilde{\sigma}$ ,  $\tilde{s}$ , and  $\varphi$ , that is,  $d\sigma = h_{\sigma}(\tilde{\sigma}, \tilde{s}) d\tilde{\sigma}$ .

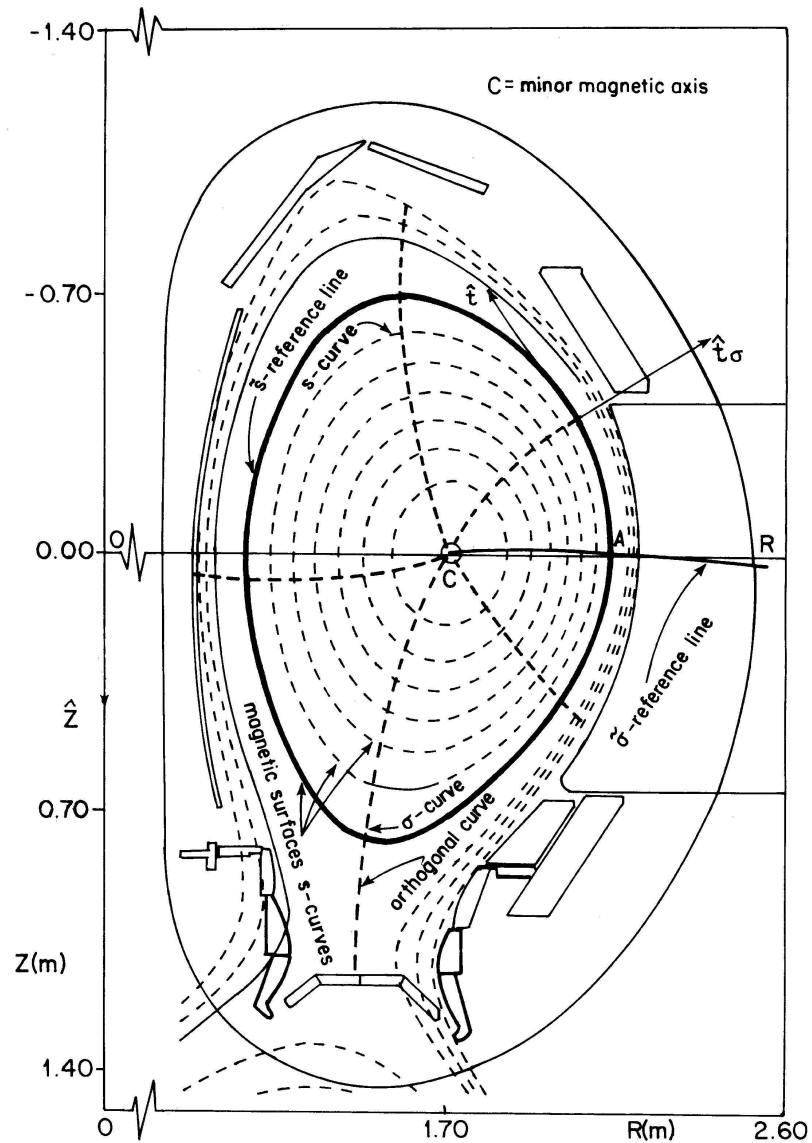


Figure 1: Cross section of the tokamak magnetic surface showing the reference curves for the coordinates used in the text.

---

The function  $\tilde{F}(\psi)$  or  $F(\tilde{\sigma})$  is a conserved function around a magnetic surface, in the same sense that pressure is a conserved function on a magnetic surface, if the nonlinear terms in the momentum equation were neglected. The new feature is that now  $F(\vec{v}, \rho, T, v)$  is a combination of velocity and position-dependent functions.

Now from the condition

$$\nabla \times \nabla F(\tilde{\sigma}) = 0 \quad ,$$

and

$$\nabla \times \left[ \frac{\partial F(\tilde{\sigma})}{\partial \sigma} \hat{n} \right] = 0 \quad ,$$

it is obtained

$$\frac{\partial F(\tilde{\sigma})}{\partial \sigma} = \left[ \frac{\partial F(\tilde{\sigma})}{\partial \sigma} \right]_1 \exp \left( - \int_0^s \kappa_\sigma ds \right) \quad ,$$

---

Here the subscript 1 denotes one point on the magnetic surface, which would be conveniently taken as the most outward point in the middle plane. The integration has to be performed along any magnetic surface curve in a  $\phi$ -constant cross section.

The above exponential appears very often in the next section and it is useful to denote it by  $\tilde{\mu}$ , that is,

$$\tilde{\mu} = \exp \left( - \int_0^s \kappa_\sigma \, ds \right) .$$

To study diffusion in the scrape off-layer (SOL) surface, the normal velocity will be

$$\bar{v} = \left( \oint R \, ds \right)^{-1} \oint \left( -\eta_\perp \frac{\partial F}{\partial \sigma} - E_p B_\phi + E_\phi B_p \right) B^{-2} R \, ds .$$

By using the continuity equation

$$\nabla \cdot \vec{j} = 0 ,$$

as well as the univalue for the electric potential  $\phi(\vec{r}, t)$ , the value of the parallel velocity can be obtained as

$$\dot{j}_{||} = - \frac{\rho B_{\phi}}{c B B_p} \frac{\partial F}{\partial \sigma} + G(\tilde{\sigma}) B ,$$

where

$$G(\tilde{\sigma}) = \left[ \oint \frac{\rho B_{\phi}}{B_p^2} \frac{\partial F}{\partial \sigma} ds + \frac{1}{\eta_{||}} \oint \frac{E_{\phi} B_{\phi}}{B_p} ds \right] / \left( \oint \frac{B^2}{B_p} ds \right) .$$

Here the density around a magnetic surface is difficult to determine, however for some simplified cases,  $\rho(\psi)$  is given by

$$\rho(\psi) = \rho_0(\psi) \exp(\omega^2 \gamma^2 / 2T)$$

where  $\psi$  is the poloidal magnetic flux. If  $\omega$  is neglected as we did at the beginning, then  $\rho$  will be constant on a magnetic surface.

In any case  $\rho$  could be also treated as an average value  $\bar{\rho}$  for each magnetic surface, that is

$$G(\tilde{\sigma}) = \left[ \bar{\rho} \oint \frac{B_\varphi}{B_p^2} \frac{\partial F}{\partial \sigma} ds + \frac{1}{\eta_{||}} \oint \frac{E_\varphi B_\varphi}{B_p} ds \right] / \left( \oint \frac{B^2}{B_p} ds \right) .$$

Finally using all our previous approximations the average normal velocity  $\bar{v}$  will be

$$\bar{v} = -\frac{\bar{\rho} \eta_\perp}{B_{\varphi_1}^2} \left( \frac{\partial F}{\partial \sigma} \right) \frac{1}{\tilde{I}_0} \left[ \frac{\tilde{I}_1}{\tilde{R}_1^2} + \frac{\eta_{||}}{\eta_\perp \tilde{\gamma}_1 \tilde{R}_1^2} \left( \tilde{I}_3 - \frac{\tilde{I}_1^2}{\tilde{I}_4} \right) \right] - \frac{E_{\varphi_1}}{B_{\varphi_1} \tilde{\gamma}_1 \tilde{I}_0} \left[ \tilde{I}_7 - \frac{\tilde{I}_1 \tilde{I}_6}{\tilde{I}_4} + \tilde{\gamma}_1^2 \tilde{I}_5 \right] ,$$

where  $R_m$  is the major radius of the minor axis, and

$$\gamma_1 = \frac{B_{p_1}}{B_{\varphi_1}} , \quad \tilde{R} = \frac{R}{R_m} , \quad d\hat{s} = \frac{ds}{R_m} .$$

All the previous integrals are written in a dimensionless way as

$$\tilde{I}_0 = \oint \tilde{R} d\hat{s} ,$$

$$\tilde{I}_1 = \oint \tilde{R} \mu(s)^{-1} d\hat{s} ,$$

$$\tilde{I}_2 = \oint \tilde{R}^3 \tilde{\mu}(s) (1 + \tilde{\gamma}_1^2 \tilde{\mu}(s)^2)^{-1} d\hat{s} ,$$

$$\tilde{I}_3 = \oint \tilde{R}^3 (1 + \tilde{\gamma}_1^2 \tilde{\mu}(s)^2)^{-1} \tilde{\mu}(s)^{-1} d\hat{s} ,$$

$$\tilde{I}_4 = \oint (1 + \tilde{\gamma}_1^2 \tilde{\mu}(s)^2) \tilde{\mu}(s)^{-1} \tilde{R}^{-1} d\hat{s} ,$$

$$\tilde{I}_5 = \oint (1 + \tilde{\gamma}_1^2 \tilde{\mu}(s)^2)^{-1} \tilde{\mu}(s) \tilde{R} d\hat{s} ,$$

$$\tilde{I}_6 = \oint \tilde{\mu}(s)^{-1} \tilde{R}^{-1} d\hat{s} ,$$

$$\tilde{I}_7 = \oint (1 + \tilde{\gamma}_1^2 \tilde{\mu}(s)^2)^{-1} \tilde{\mu}(s)^{-1} \tilde{R} d\hat{s} .$$

## RESULTS

As in previous work in order to perform the diffusion calculation including non-linear flows, the family of selected magnetic surfaces will be identify by the equations

$$\tilde{R}(\lambda, \theta) = \frac{R(\lambda, \theta)}{R_m} = 1 + \tilde{a} \lambda \cos \theta - \lambda^2 \left[ \tilde{\Delta} + \frac{\tilde{a} T(a)}{4} (1 - \cos 2\theta) \right] ,$$

$$\tilde{z}(\lambda, \theta) = \frac{z(\lambda, \theta)}{R_m} = \tilde{a} \lambda E(a) \sin \theta - \frac{\lambda^2 \tilde{a} E(a) T(a)}{4} \sin 2\theta ,$$

where  $\lambda$  is a parameter identifying each magnetic surface, and here all the quantities and variables with tilde are dimensionless, that is

$$\tilde{a} = \frac{a}{R_m} , \quad \tilde{\Delta} = \frac{\Delta(a)}{R_m} .$$

The symbol  $E(a)$  and  $T(a)$  denote the elliptic and triangularity distortion, respectively.

As in a previous work it is convenient to define also dimensionless velocity as

$$\tilde{v} = \frac{\bar{v}}{\bar{v}_{oc}} ,$$

where  $\bar{v}_{oc}$  is the normal velocity when ellipticity and triangularity are zero, that is,

$$\bar{v}_{oc} = - \frac{\eta_{\perp} \bar{\rho}}{B_{\varphi_1}^2} \left( \frac{\partial F}{\partial \sigma} \right)_1 \alpha_0 \quad ,$$

and  $\alpha_0$  is defined by

$$\alpha_0 = \frac{\tilde{I}_2(0)}{\tilde{R}_1^2} + \frac{\eta_{||}}{\eta_{\perp}} \frac{1}{\tilde{R}_1^2 \tilde{\gamma}_1^2} \left( \tilde{I}_3(0) - \frac{\tilde{I}_1(0)^2}{\tilde{I}_4(0)} \right) \quad .$$

Circular magnetic surface are denoted with the number zero.

Dimensionless inductive electric field is also used and defined as

$$\tilde{E}_{\varphi_1} = \frac{E_{\varphi_1}}{- \frac{\eta_{\perp} \bar{\rho}}{B_{\varphi_1}^2} \left( \frac{\partial F}{\partial \sigma} \right)_1} \quad .$$

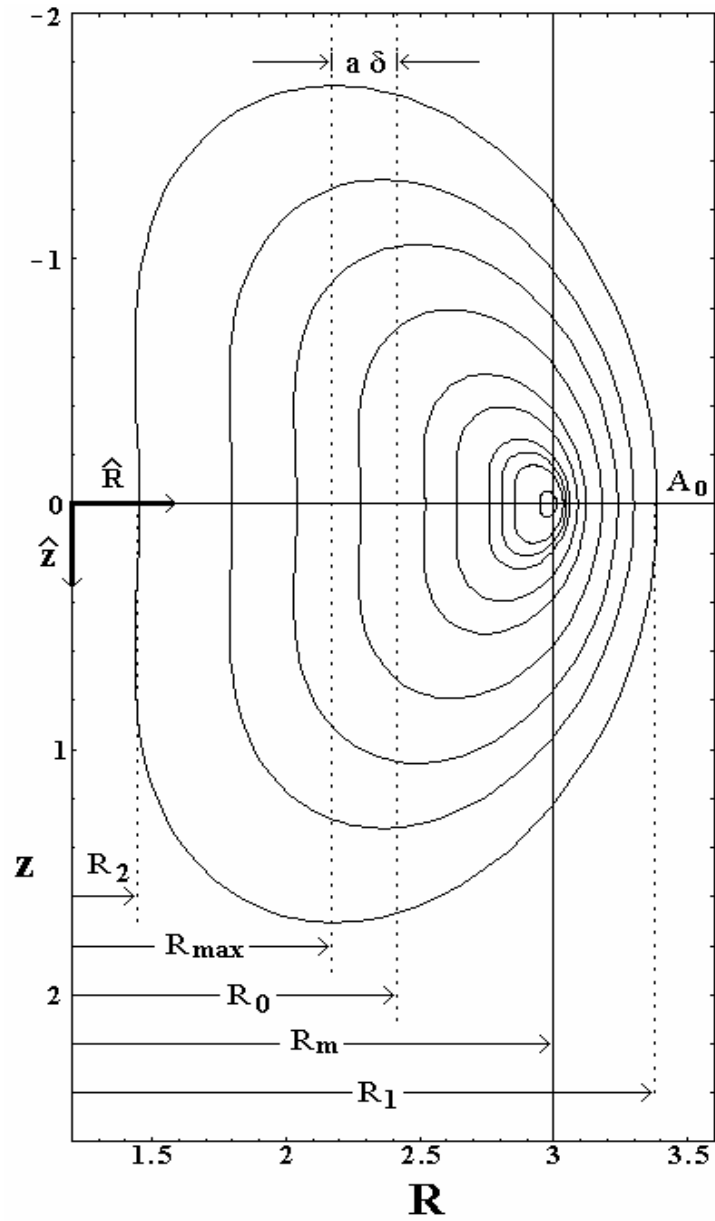


Figure 2: Illustrative figure showing the main parameters used in the equations for the family of magnetic surfaces.

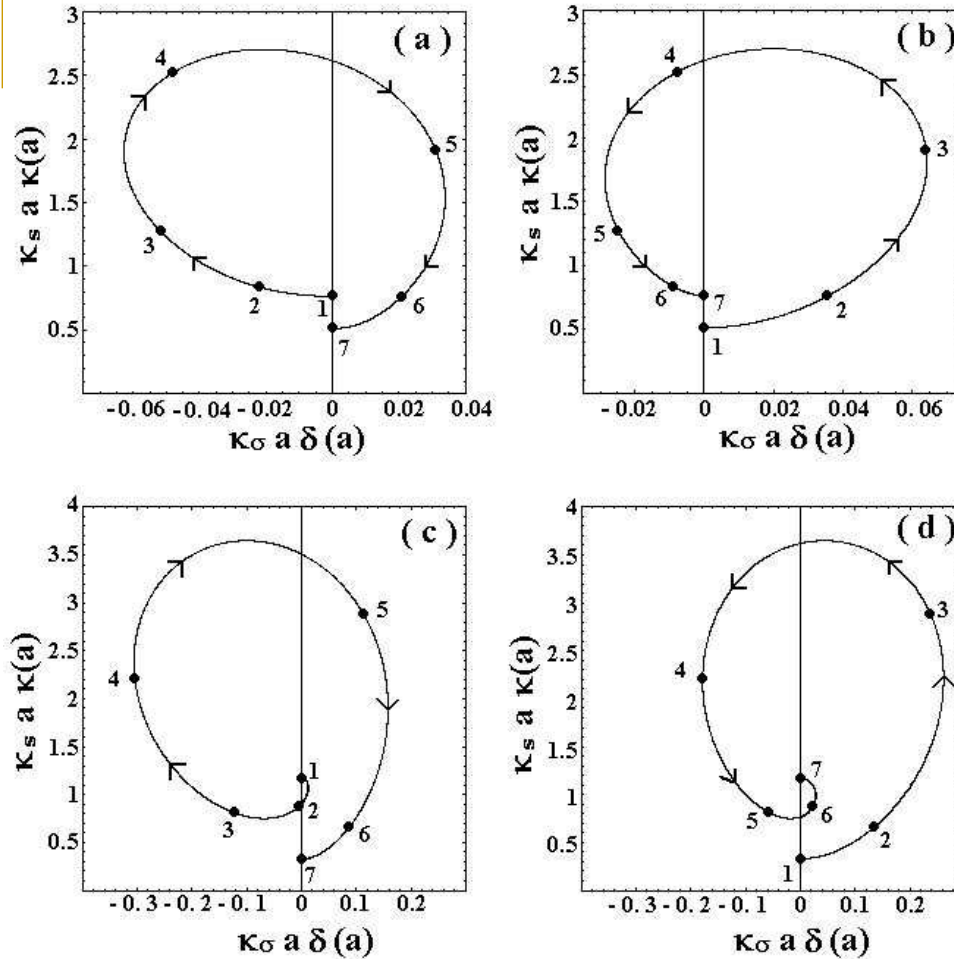


Figure 3: Dimensionless geodesic curve  $\kappa_s$  vs. normal curvature, scales with the factor  $a \kappa(a)$  and  $a \delta(a)$ , respectively. The points show values of  $\theta$  every  $30^\circ$ , starting with  $\theta = 0^\circ$ . The arrows illustrate the rotation sense.

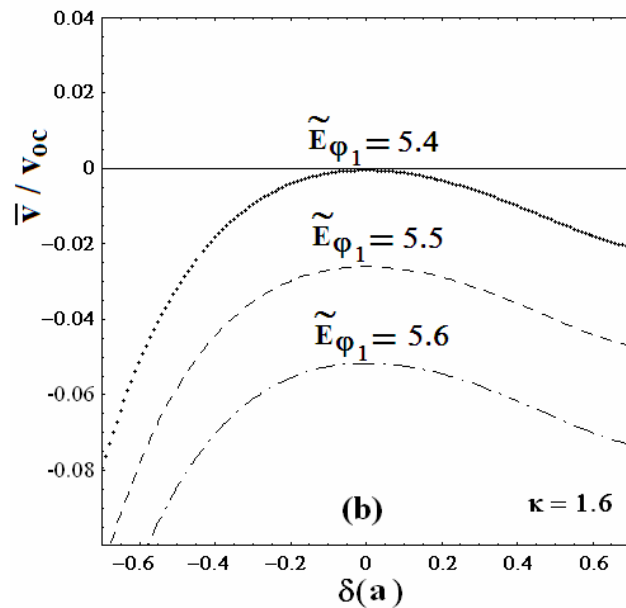
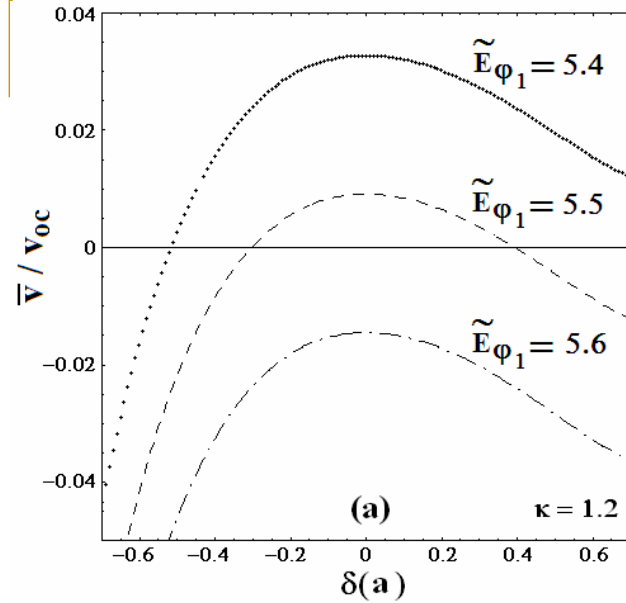


Figure 4: Dimensionless diffusion velocity versus triangularity for three different dimensionless inductive fields  $\tilde{E}_{\varphi_1} = 5.4$  (point line), 5.5 (dash line) and 5.6 (dash-point line). Fig.(1a) and (1b) are respectively for elongations  $\kappa(a) = 1.2$  and 1.6

---

In figure 4, the dimensionless velocities are shown as a function of the triangularity for three different values of dimensionless electric field and for a given elliptic elongation, which are 1.2 and 1.6, in Figure 3a and 3b, respectively.

These results show that positive and negative triangularities increase confinement. Since confinement corresponds to negative values of diffusion velocity. The points where the velocities are zero, correspond to marginal confinement, that is, to zero diffusion velocity. The worst situation is just at the maximum of the curves, which is usually near  $\delta(a) \cong 0$ , though not always exactly for zero triangularity. There are in general better confinement with negative triangularities than with positive ones, since for the same absolute value of triangularities the absolute value of the negative velocities are larger in the negative side of  $\delta(a)$ . Furthermore the triangularity tends to a plateau for positive large values of  $\delta(a)$ , and that plateau does not appear in the negative side of  $\delta(a)$  at least for the range of parameters here investigated.

---

Ellipticity is also important in confinement, as can be seen looking at the previous figures. There is better confinement for elliptic elongation  $\kappa(a) = 1.6$  than for  $\kappa(a) = 1.2$ . However, in this work the analysis is carried out mainly on triangularity effects. Here, we are also interested in finding out the differences in diffusion due to current holes. In this case the Shafranov shift, triangularity and elliptic elongation are taken from the work of V. Yavorsky et al. Their definitions are

$$\Delta(\lambda) = \Delta_0 (1 - \lambda^2) \quad ,$$

$$\Lambda(\lambda) = \Lambda_a \lambda^2 \quad ,$$

$$k(\lambda) = k_a - (k_a - k_0)(1 - \lambda^2)^2 - 0.5 k'_a \lambda^2 (1 - \lambda^2) \quad .$$

where  $\Lambda_a$  denote the triangularity, instead of the usual notation  $\delta$ . The parameter  $\lambda$  denote as usual the magnetic surface, which is also defined as

$$\lambda = \frac{\tilde{\sigma}}{a} = \frac{r}{a}$$

---

In the above paper, a parameter  $x_m$  is introduced in order to adjust the analytic form to the experimental data. The calculation here will be carried out for the Japanese tokamak JT-60U, and for this device a good value of  $x_m$  is 0.6. This parameter determines another parameter  $m$  by

$$m = \frac{3((1-x_m)^{-6} - 1)}{(1+x_m^{-1})},$$

which is used in the analytic form for  $j_\varphi$

$$j_\varphi = (1-\lambda^2) (1-(1-\lambda)^6)^{2m}$$

This equation is well adjusted to the experimental values. Fig. 5 shows this current along the cross section.

---

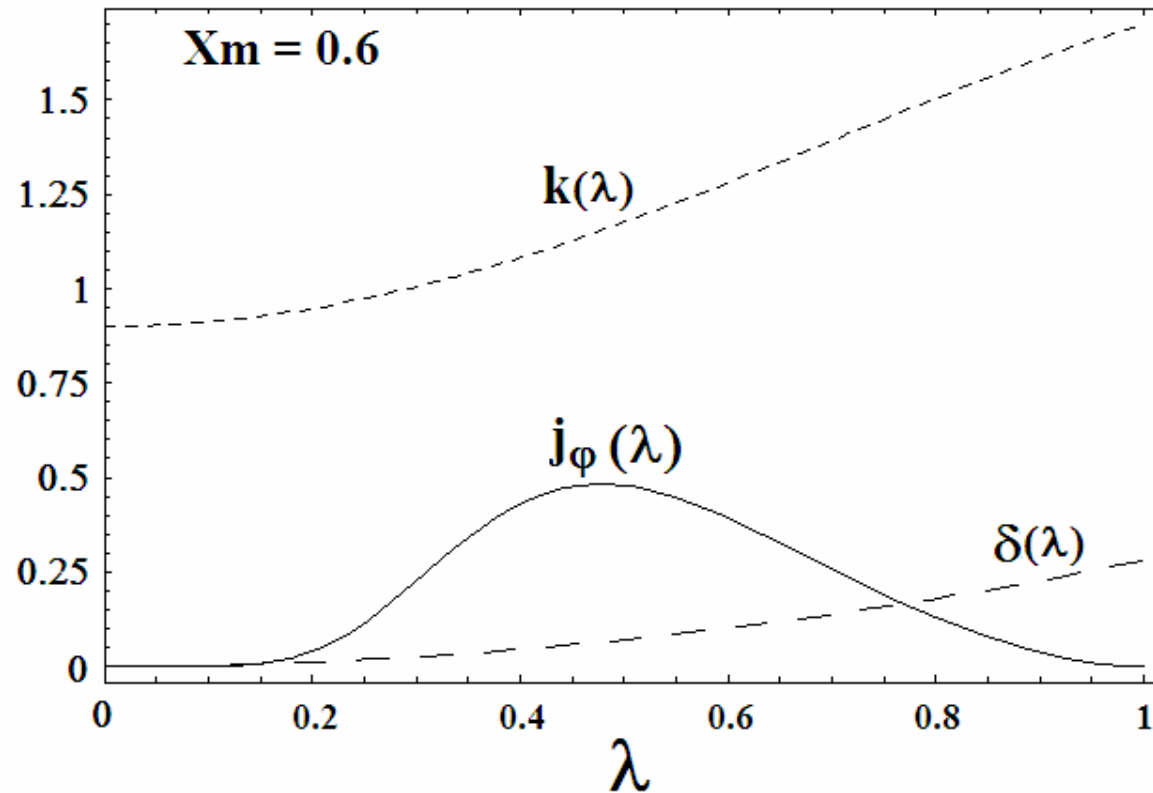


Figure 5: Current density profile, elongation and triangularity along the major radius. The parameter  $\lambda$  identifies each magnetic surface and the value of the parameter  $X_m$  is shown on upper-left corner.

---

The minor magnetic axis is as usually as  $\lambda=0$ , and the current hole is about 1/10 of the plasma size measured by  $a$ . All the previous definitions allow to determine  $K_\sigma$ , and from here our  $\mu$  parameter, corresponding to the elongation  $k(a) = 1.7$ . The dimensionless normal velocity is determined for both cases without and with current hole.

The results given in Fig.(6a) and (6b) show that there is a clear improvement in confinement for the hole effect. The patterns however are also a little different, since when the current holes are present the plateau for large positive triangularities are more ample than in the case with no hole.

The comparison between the results without or with current holes is better carried out using the marginal inductive field, that is, the values where the normal velocity are zero. These curves separate the confinement region from the no-confinement region, characterized by negative or inward diffusion velocities.

Figure 7, shows  $E_{\phi \text{ marginal}}$  as a function of triangularity for elliptic elongation  $k(a) = 1.7$ . The improvement in confinement due to the hole current is actually very important. In the worst situation for this elongation, the normal velocity is about 20 and 25 % larger when the current hole is present than where there is not hole

---

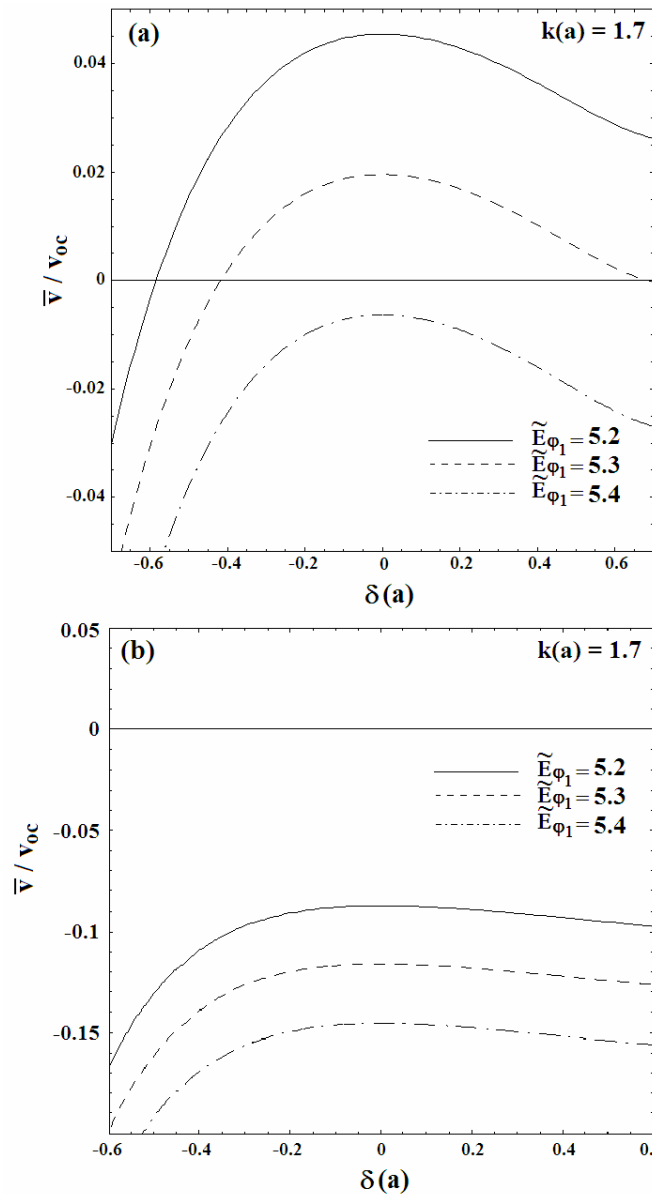


Figure 6: Dimensionless diffusion velocity versus triangularity for elongation  $k(a) = 1.7$ , in the scrape-off-layer surface, and three different dimensionless inductive fields 5.2 (plain line), 5.3 (dash Line) and 5.4 (dash-point line). Figure (6a) is for plain currents with no-holes, and Fig. (6b), when current holes are present.

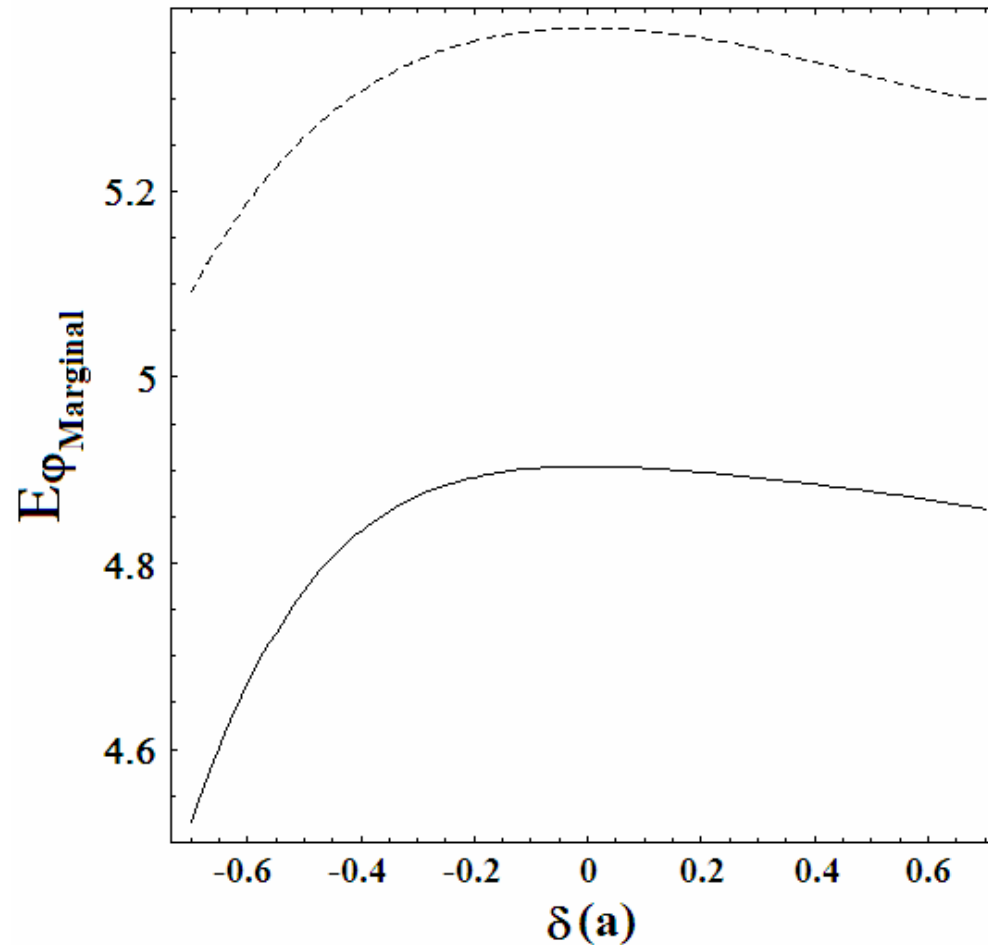


Figure 7: Marginal dimensionless inductive field as a function of triangularity for plasma configurations with current holes (plain line) and without current holes (dash line)

---

## CONCLUSION AND DISCUSSION

**1.-** Non-linear collisional transport in axisymmetric tokamaks has been analyzed including non-linear flows for toroidal plasma configurations with ellipticity and triangularity in the low vorticity limit. This generalizes previous linear treatments recently published. The normal velocity in the scrape-off-layer surface has been determined for a general plasma configuration. The results are given as a function of several integrals around some magnetic curves. Numerical calculations have been carried out using equations for the magnetic surfaces consistent with Grad-Shafranov equations, which are nonlinear in the parameter  $\lambda$ , characterizing each magnetic surface.

**2.-** Numerical calculations on diffusion velocities have been also carried out for plasma configuration with current holes, which appear in the experiments with large tokamaks. The present analysis is mainly concentrated in the effects on diffusion due to different triangularities.

---

---

**3.-** Collisional confinement improves when triangularity is present in the tokamak plasma configuration. However, the effect of negative triangularity is more significant than positive ones. In the range of parameters here analyzed (-0.6 to 0.6) a plateau tendency appears in the diffusion velocity for positive triangularities, but not for negative ones. Ellipticity is also important in confinement but a complete analysis of this matter will be carried out in future works.

4.- The influence on confinement due to current holes in the plasma is also analyzed here. The present results show slight improvement in confinement when current holes are present. In this case, the pattern of the curves looks as in the case where there is not hole, but the plateau formation for positive triangularities is clearer and with a larger extension. This effect is complementary to the increasing in confinement. Though the numerical calculations are carried out for some selected tokamaks, however the present treatment is very general, and not limited to these cases. In our analysis dimensionless variables are used most of the time in order to reach more general results, and it seems that the present work should be useful in future tokamak designs.

---